Using CombiCells, a platform enabling titration and combinatorial display of cell surface ligands, to investigate the sensitivity and costimulatory requirements of TCRs and CARs

Ashna Patel[1], Violaine Andre[1], Sofia Bustamante Eguiguren[1], Michael I. Barton[1], Eleanor M. Denham[1*], Johannes Pettmann[1†], Alexander M Mørch[2], Mikhail A. Kutuzov[1], Jesús A. Siller-Farfán[1], Michael L. Dustin[2], P. Anton van der Merwe[1], Omer Dushek[1,¶]

[1]Sir William Dunn School of Pathology, University of Oxford, Oxford OX1 3RE, UK
[2]The Kennedy Institute of Rheumatology, University of Oxford, Oxford OX3 7FY, UK
[*]Present address: Enara Bio Ltd, The Bellhouse Building, Oxford Science Park, Sanders Road, Oxford, OX4 4GD, UK
[†]Present address: GlaxoSmithKline Pharmaceuticals, Rue de l'Institut 89, 1330 Rixensart, Belgium
[¶]Corresponding author

Key words: Receptor/ligand interactions; cell-cell recognition; surface ligand presentation; T cell antigen sensitivity; T cell co-stimulation; T cell co-inhibition; chimeric antigen receptors

Pre-print server: biorxiv

Open access: This research was funded in whole, or in part, by the Wellcome Trust [207537/Z/17/Z]. For the purpose of Open Access, the authors have applied a CC BY public copyright licence to any Author Accepted Manuscript version arising from this submission.

Abstract

Receptor/ligand interactions at cellular interfaces are ubiquitous and the integrated signals from multiple interactions determines cellular decision-making. However, our understanding of cell-cell recognition is hampered by the inherent difficulty in precisely controlling the density of cell-surface ligands. Here, we adapt the protein Spycatcher, which forms a spontaneous covalent bond with Spytag, to enable the presentation of native ligands on cells. By expressing Spycatcher on the surface of cells using a short membrane-anchoring hinge, we show that addition of different concentrations/combinations of purified Spytag-ligands allows for the combinatorial display of ligands on cells (CombiCells) within minutes. We demonstrate the utility of the platform by quantifying T cell antigen sensitivity and the contribution of the CD2, LFA-1, CD28, and PD-1 accessory receptors. We show that T cell recognition of pMHC antigens is enhanced mostly by CD2/ligand engagement whereas recognition of the antigen CD19 by CAR-T cells is enhanced mostly by LFA-1/ligand engagement. Moreover, we show that PD-1/ligand engagement can inhibit T cell activation triggered solely by TCR/pMHC interactions, as well as the amplified activation induced by CD2 and CD28 co-stimulation. The ability to easily produce cells with different concentrations and combinations of ligands should accelerate our understanding of how receptor/ligand interactions at cellular interfaces control cellular decisions.

Graphical abstract

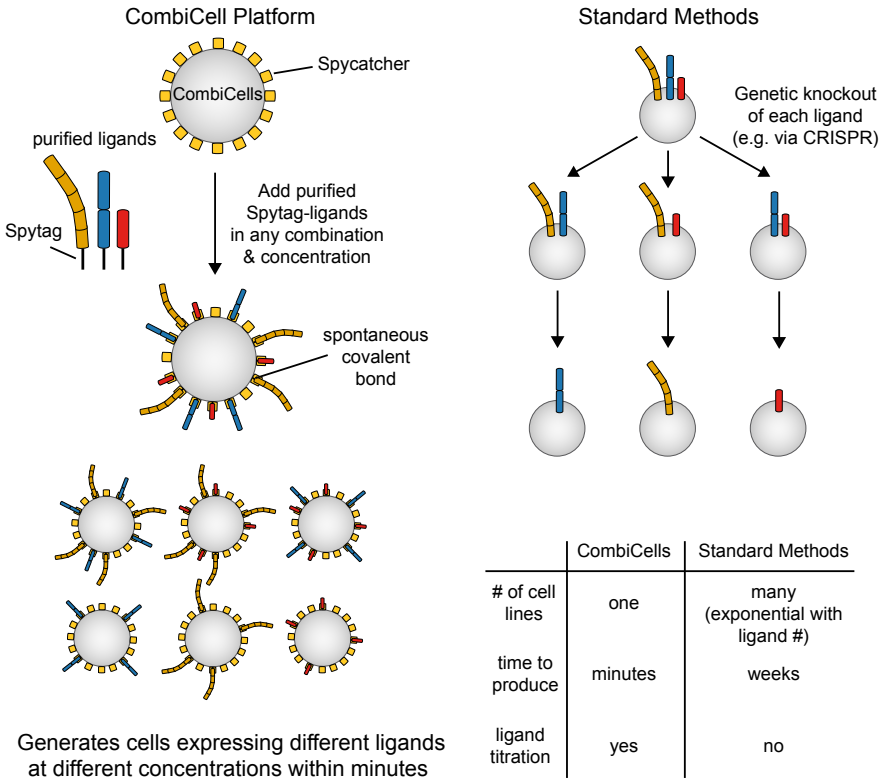

	CombiCells	Standard Methods
# of cell lines	one	many (exponential with ligand #)
time to produce	minutes	weeks
ligand titration	yes	no

Introduction

Direct cell-cell communication is a ubiquitous and essential process in multicellular organisms. It is critical during development and tissue maintenance, and underlies the proper functioning of the nervous and immune systems (1). Communication at cellular interfaces relies on diverse families of surface receptors that transduce signals upon recognising their ligands on the surface of other cells. When studying surface receptors that recognise ligands in solution (e.g. G-Protein Coupled Receptors, Receptor Tyrosine Kinases, and Cytokine Receptors), it is trivial to experimentally vary the concentration and combination of soluble ligands. In contrast, it is far more challenging to vary the concentration and combination of cell surface ligands. This technical limitation has hampered our ability to understand cell-cell recognition.

Arguably the most well studied form of cell-cell recognition is T cell antigen recognition. T cells continuously patrol and scan cells throughout the body, seeking abnormal antigens derived from pathogens and mutated proteins produced by cancer cells. T cell activation hinges on whether their T cell antigen receptors (TCRs) bind these antigens, usually in the form of peptides presented on major-histocompatibility-complexes (pMHCs). Crucially, the response of the T cell also depends on engagement of other 'accessory' receptors which can enhance or inhibit the response (2). Infected or cancerous cells can evade immune recognition by reducing the level of antigen they express on their cell surface. For example, relapses following chimeric antigen receptor (CAR)-T cell therapy are associated with decreases in levels of the target antigen CD19 on the surface of cancer cells (3). In addition, pathogen-infected and cancerous cells can evade immune recognition by changing the levels of ligands to accessory receptors (4–6). It follows that it is important to be able to investigate how T cell activation is regulated by the concentration of antigens and the combinations of accessory receptor ligands on the target cells.

The accessory receptors CD2, LFA-1, and CD28 are known to enhance T cell responses mediated by the TCR, but their contribution to T cell responses mediated by CARs remains unclear. This is challenging to study as it is difficult to manipulate the surface levels of CAR and accessory receptor ligands. Current methods rely on laborious genetic methods to produce cell lines with desired combinations/surface densities of the required ligands. However, the number of cell lines needed increases exponentially with the number of ligands and surface densities, if all combinations are to be tested, making such experiments impractical. Moreover, the method is susceptible to genetic drift between these cell lines, raising doubts as to whether any differences observed are actually the result of differences in ligand expression.

Here, we introduce a novel platform enabling the rapid production of cells expressing any combination and concentration of ligands, and we use it to study T cell activation via a native TCR or synthetic CARs and the contribution of accessory receptors.

Results

The purified extracellular domain of native ligands fused to Spytag can readily couple to cell surface Spycatcher

To enable the combinatorial display of ligands on cells (CombiCells), we reasoned that cell surface expression of the protein Spycatcher, which forms a spontaneous covalent bond with a peptide tag (Spytag) (7), could be used to couple the extracellular domain of purified ligands fused to Spytag (Fig. 1A). Con-

sequently, we fused the C-terminus of Spycatcher to the extracellular hinge of human CD52 (hCD52; 7 aa), murine CD80 (mCD80; 20 aa), or a variant of mCD80 that contained fewer residues (mCD80-short; 6 aa). The rationale for coupling the C-terminus of Spycatcher to these short hinges is that it would be expected to maintain a compact conformation bringing Spytag fusion proteins close to the membrane. The CD52 and CD80 hinges are anchored to the cell surface through glycosylphosphatidylinositol (GPI) and a transmembrane domain, respectively. We transduced these surface Spycatchers into CHO-K1 cells and detected expression by coupling a purified fluorescent protein fused to Spytag (Spytag-mClover3, Fig. 1B). A titration of Spytag-mClover3 revealed that the hCD52 hinge surface Spycatcher expressed at the highest level and that saturation was achieved at approximately 1 μM of Spytag-mClover3. Lastly, all surface Spycatchers were mobile with typical diffusion coefficients for membrane proteins (Fig. 1C). Given its higher expression, we used surface Spycatcher fused to the hinge of hCD52 for subsequent experiments.

T cell activation is known to be controlled in part by the accessory receptors CD2, LFA-1, and CD28, whose ligands are CD58, ICAM-1, and CD86 (or CD80), respectively. To study their individual contributions using surface Spycatcher, a target cell that does not express these ligands is required. Given that CHO-K1 cells are hamster ovary cells, they are not expected to express these ligands with the exception of ICAM-1, which has been shown to be functional (8). Therefore, we used CRISPR to knockout hamster ICAM-1 before transducing surface hCD52-Spycatcher (Fig. 2A,B). We coupled purified Spytag-mClover3 and confirmed that it remained mobile on the cell surface (Fig. 1D). We refer to these CHO-K1 ICAM-1^{-} hCD52-Spycatcher^{+} as CHO-K1 CombiCells.

We next designed constructs that contained the full extracellular domains of CD58, ICAM-1, CD80, and CD86 fused to a C-terminal Spytag (for coupling to Spycatcher) and Histag (for purification). We produced and purified these ligands and coupled them to CHO-K1 CombiCells before measuring their surface levels using flow cytometry (Fig. 2C). We found that each ligand can be coupled at levels $\gtrsim$10-fold higher than those found on the T2 cell line, other cell lines, and primary T cells and macrophages (Fig. 2D). Indeed, the absolute number of ligands that can be coupled exceeded $\sim 10^6$ per cell (Fig. 2E). Lastly, we found that coupled ligands had a cell surface lifetime of $\approx$7 hours (Fig. 2F, Fig. S1).

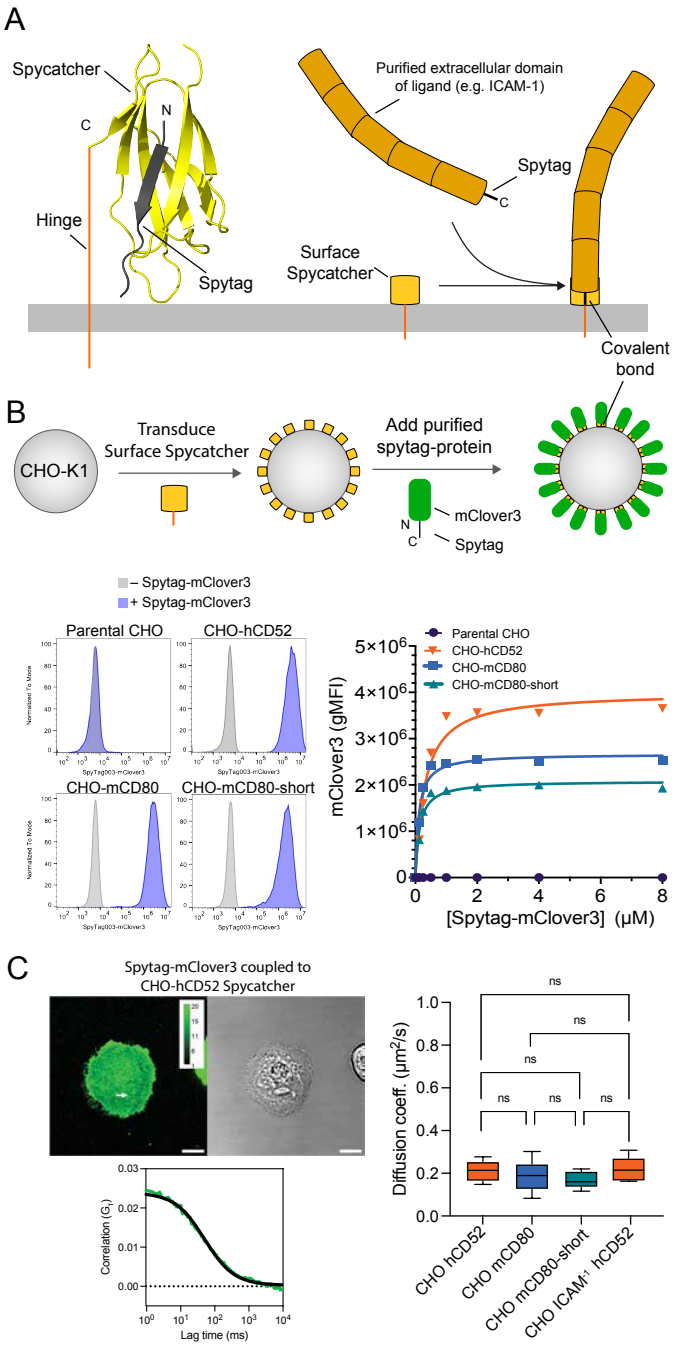

Figure 1: **Spycatcher can be expressed on the cell surface and remain mobile when coupled to a purified fluorescent protein fused to Spytag. (A)** Left: Structure of Spycatcher (yellow) coupled to Spytag (black) indicating the location of the hinge for surface display (C-terminus of Spycatcher) and the location of the extracellular domain of ligand (N-terminus of Spytag). Structure taken from PDB:4MLI. Right: Schematic of purified protein fused to Spytag coupling to surface Spycatcher. **(B)** CHO-K1 cells transduced with surface Spycatcher were coupled with purified mClover3 fused to Spytag and detected in flow cytometry. **(C)** Scanning fluorescent correlation spectroscopy (sFCS) is used to determine the diffusion coefficient of surface Spycatcher. Representative confocal image of Spytag-mClover3 coupled to surface Spycatcher acquired in photon-counting mode (top left). Calibration bar indicates photons per pixel and white arrow indicates position of the sFCS line (scale bar = 10μm). Representative spatially-averaged auto-correlation from a single cell is fit to determine the diffusion coefficient (bottom left; data - green, model fit - black). The diffusion coefficients of Spytag-mClover3 coupled to the indicated surface Spycatcher on CHO-K1 cells (right).

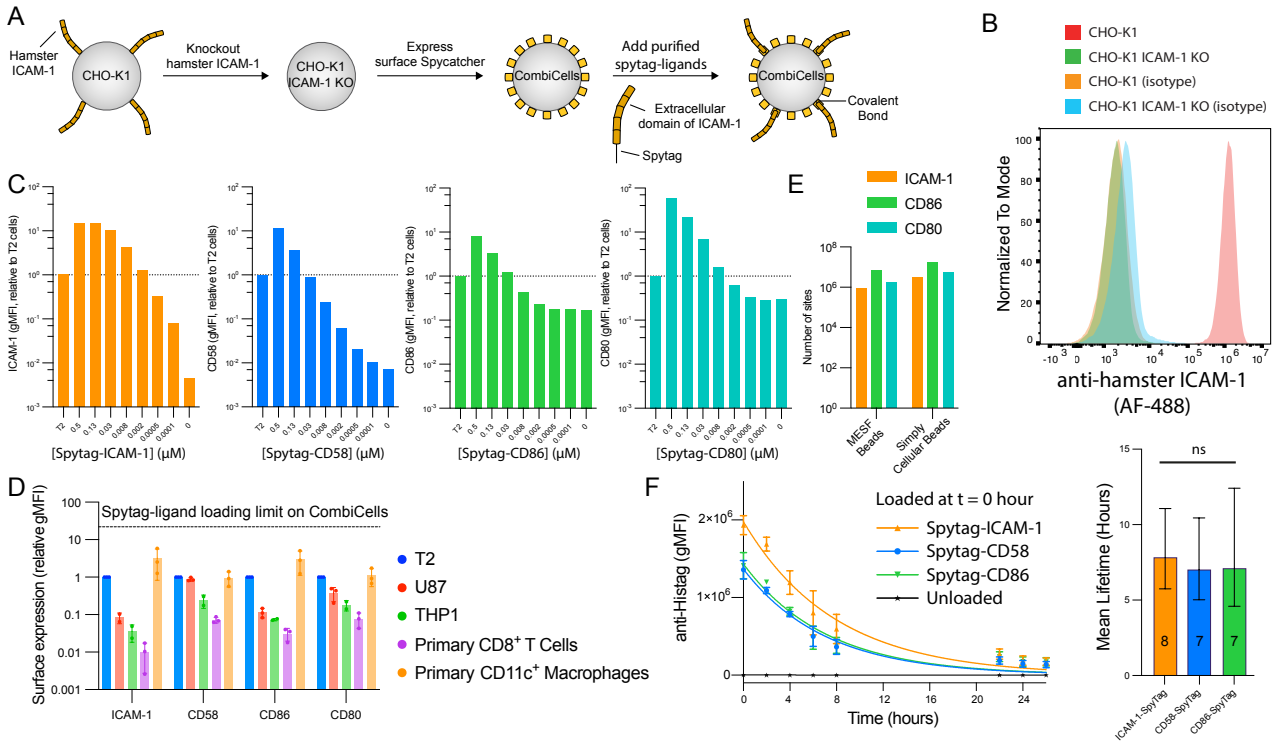

Figure 2: **Purified ligands to prominent T cell accessory receptors fused to Spytag can readily couple to surface Spycatcher on CHO-K1 ICAM-1 KO cells. (A)** Experimental workflow. **(B)** Surface expression of hamster ICAM-1 on the indicated CHO-K1 cell line. **(C)** Expression of the indicated ligand on CHO-K1 CombiCells (coupled to Spycatcher) relative to native expression on T2 cells (horizontal line) detected by flow cytometry. **(D)** Expression of the indicated ligands on different cells relative to T2 cells. **(E)** The absolute number of the indicated ligand per cell when coupled at 0.5 μM determined using the indicated calibration method. **(F)** CHO-K1 CombiCells were loaded with 0.1 μM of ligand and surface levels were measured over time (left). An exponential fit is used to determine the mean lifetime (right) and compared using a one-way ANOVA.

The accessory receptor CD2 primarily controls the sensitivity of a pMHC targeting TCR and CAR

To study the impact of accessory receptor ligands on T cell antigen sensitivity, we produced purified Spytag-pMHC by refolding HLA-A*02:01 fused to Spytag with β2m and a peptide from the NY-ESO-1 cancer antigen (Fig. 3A). We performed a preliminary experiment by co-culturing primary human CD8+ T cells expressing the NY-ESO-1 specific 1G4 TCR (9) with CHO-K1 CombiCells loaded with different concentrations of Spytag-pMHC and each ligand. We first confirmed that the surface level of Spytag-pMHC can be varied without impacting the surface level of each Spytag-ligand (and vice versa) and found this to be the case provided that the total concentration of Spytag-proteins remained below 1 μM, which was the maximum concentration of Spytag-proteins used (Fig. 3B). We measured T cell activation by surface markers (4-1BB, CD69) and by secreted cytokines (IL-2, IFN-γ, and TNF-α) (Fig. 3C, Fig. S3). We observed the expected increase in T cell activation with increasing concentrations of Spytag-pMHC and with increasing concentration of each Spytag-ligand, consistent with the co-stimulation function of LFA-1, CD2, and CD28. Therefore, this preliminary experiment confirmed that T cells can exploit Spytag-ligands to accessory receptors in recognising Spytag-pMHC in a concentration-dependent manner.

We note that the impact of adding Spytag-ICAM-1 on T cell activation is largely absent on the parental CHO-K1 cell line prior to hamster ICAM-1 knockout (Fig. S2). This underlines the importance of removing endogenous ligands and suggests that T cells can exploit endogenously expressed ligands when recognising Spytag-antigens presented on surface Spycatcher.

To directly compare the antigen sensitivity of the 1G4 TCR and a CAR, we used the D52N 2nd generation CAR (CD28 hinge, transmembrane, and co-stimulation domain fused to the ζ-chain), that also recognises the NY-ESO-1 pMHC antigen (10) (Fig. 4A). We found that both antigen receptors expressed at similar levels (Fig. 4B). We prepared CHO-K1 CombiCells with different concentrations of antigen alone or in combination with a fixed concentration of each co-stimulation ligand before measuring surface markers (4-1BB, CD69), cytokines (IL-2, IFN-g, TNF-a), and TCR/CAR downregulation (Fig. 4C-E, Fig. S4).

In the case of the TCR, we found that all accessory receptors acted as co-stimulation molecules but with different quantitative phenotypes. We found that CD2 increased antigen efficacy (E_{max}) and sensitivity (P_{50}) for all cytokines and surface markers, and also increased TCR downregulation, and did so with the largest quantitative effect. LFA-1 increased antigen sensitivity for surface markers and increased TCR downregulation, albeit with a smaller fold-change compared to CD2, but had no impact on cytokines. Lastly, CD28 primarily increased antigen efficacy for IL-2 but had largely no other phenotype. Taken together, these results highlight that CD2 has a broader and larger impact on both antigen sensitivity and efficacy over a broad range of responses from expanded human $CD8^+$ T cells. In the case of the CAR, we found a similar qualitative pattern with CD2 imparting the largest co-stimulation effect. However, the quantitative impact was much more modest, with antigen sensitivity improving by 11 and 3.9-fold for 4-1BB and IL-2, respectively, compared to 230 and 46-fold for the TCR. As a result, the fold-difference in antigen sensitivity between the TCR and CAR increased from 30-fold when recognising antigen alone to 300-fold or 120-fold when recognising antigen in the presence of ligands for CD58 or LFA-1, respectively. The lack of any impact of extrinsic CD28 on CAR cytokine production (Fig. 4E) was not unexpected given that it already contained intrinsic CD28 co-stimulation.

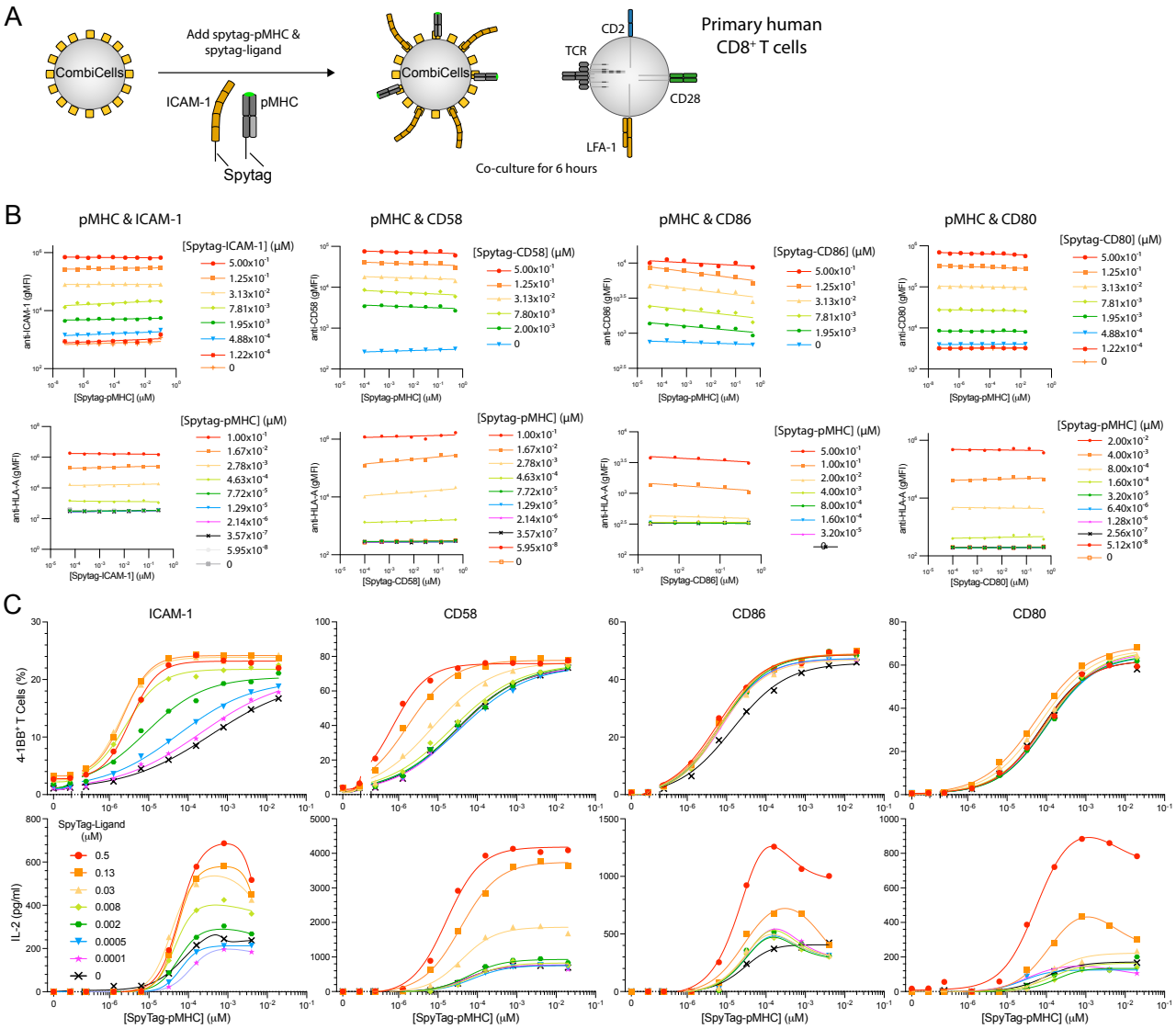

Figure 3: **T cell activation is determined by the combinatorial display of ligands. (A)** Experimental workflow. **(B)** Surface level of the indicated ligand (top row) and pMHC (bottom row) detected by flow cytometry after coupling the indicated combination of ligand and pMHC. **(C)** T cell activation measured by surface 4-1BB (top row) or supernatant IL-2 (bottom row) after 6 hours of co-culture with CombiCells (Fig. S3 for additional activation data). Experiments in each column of B and C were performed independently by transducing primary human CD8+ T cells isolated from different leukocyte cones.

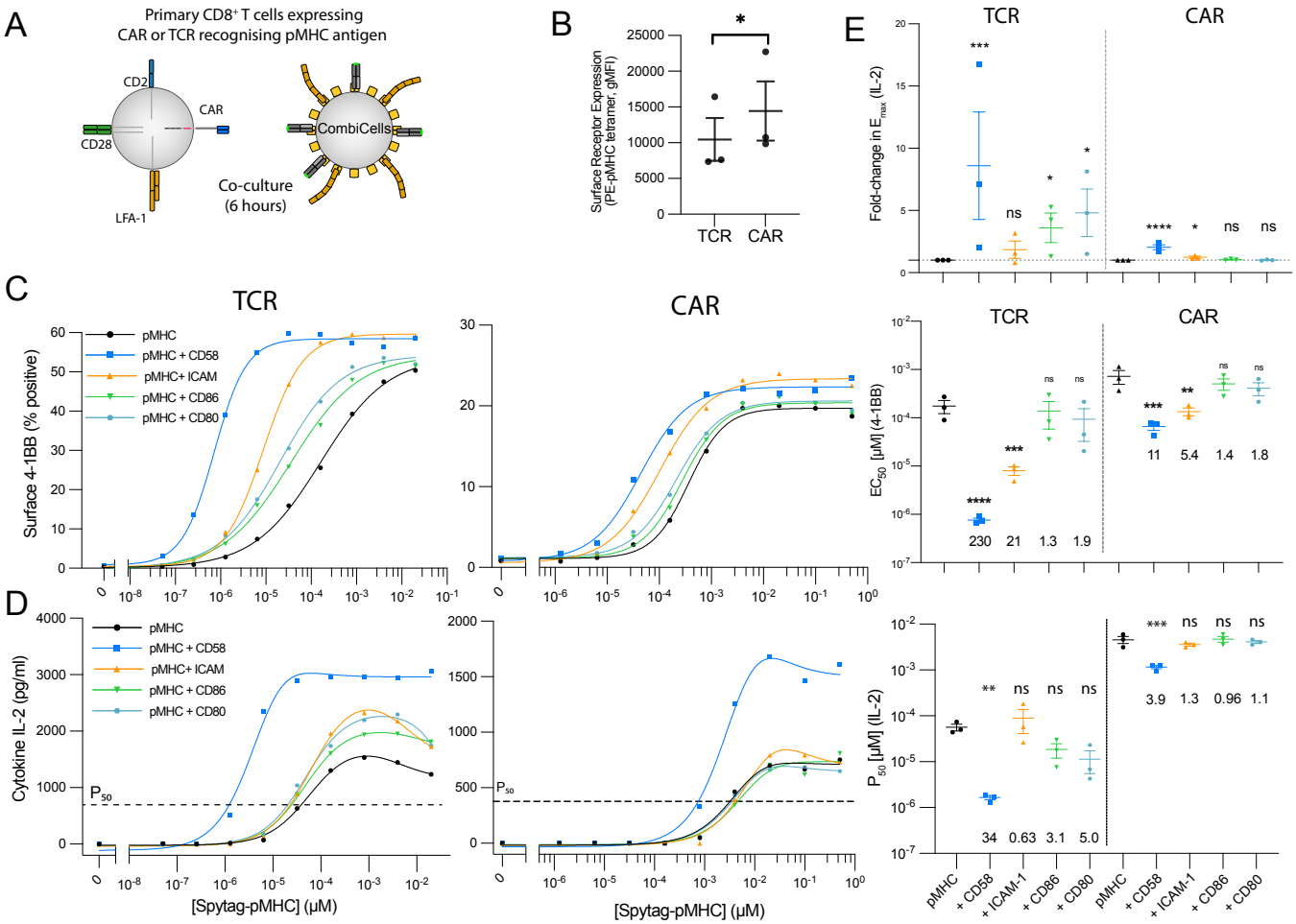

Figure 4: **The TCR is more efficient than the CAR at exploiting CD2 and LFA-1 to increase antigen sensitivity.** **(A)** Schematic of assay. **(B)** Surface antigen receptor assessed using pMHC tetramer. **(C,D)** Representative dose-response for the TCR and CAR (left) and summary measures of antigen sensitivity across N=3 independent experiments (right). **(E)** The fold-change in the maximum IL-2 secreted relative to pMHC alone. See Fig. S4 for additional measures of T cell activation. A paired t-test (B) or a t-test with Dunnett's multiple comparison correction on log-transformed values (C,D,E) is used to determine p-values. Abbreviations: * = p-value≤0.05, ** = p-value≤0.01, *** = p-value≤0.001, **** = p-value≤0.0001.

The accessory receptor LFA-1 primarily controls the sensitivity of CD19 targeting CARs

We next investigated the antigen sensitivity of two clinically-approved CAR-T cell therapies targeting the folded antigen CD19 on the surface of B cells: Yescarta and Kymriah. These 2nd generation CARs use the same FMC63 recognition domain but rely on either CD28 hinge, transmembrane, and co-stimulation (Yescarta) or CD8 hinge and transmembrane with 4-1BB co-stimulation (Kymriah). The current method to study CAR-T cell antigen sensitivity is to generate panels of cells expressing different levels of the antigen (11, 12). Using a panel of the B cell leukemia Nalm6 cell lines, we found T cell activation was already maximal in response to the clone with the lowest CD19 levels, barely detectable by flow cytometry (Fig. S5). Similarly, T cell activation is observed at pMHC concentrations $<10^{-5}$ μM (Fig. 3C) whereas detection of pMHC by flow cytometry requires concentrations $>10^{-4}$ μM (Fig. 3B). This inability to measurably vary antigen surface densities in the relevant functional range when using cell lines highlights the need for antigen titrations to quantify T cell sensitivity.

In order to titrate CD19 on target cells, we produced Nalm6 CombiCells by transducing hCD52-Spycatcher into CD19 KO Nalm6 cells (Fig. 5A) and confirmed that purified Spytag-CD19 can readily couple to the cell surface (Fig. 5B). The surface expression of CD19 remained stable for over 24 hours on Nalm6 CombiCells with a lifetime of 49 hrs (Fig. 5C). Interestingly, surface expression of SpyTag-CD19 was less stable on CHO-K1 CombiCells or the U87 glioblastoma cell line expressing hCD52-Spycatcher (Fig. 5C).

When Nalm6 CombiCells were loaded with a range of concentrations of Spytag-CD19 and used to stimulate primary $CD8^+$ T cells expressing either CAR, the antigen sensitivity of Yescarta was 6.3 to 11.5-fold higher than Kymriah (Fig. 5D). T cell activation, as measured by 4-1BB surface expression, was detected even when CD19 levels on the Nalm6 surface were too low to detect (Fig. 5D, black arrow). To investigate the contribution of accessory receptors, we used the CHO-K1 CombiCell assay (Fig. 5E). In contrast to pMHC-targeting TCR and CAR, we found that the antigen sensitivity of these CD19-targeting CARs was enhanced more by LFA-1 than by CD2 ligands (Fig. 5F). This suggests that CD2 is not being efficiently exploited by the CD19 CARs currently licensed for clinical use.

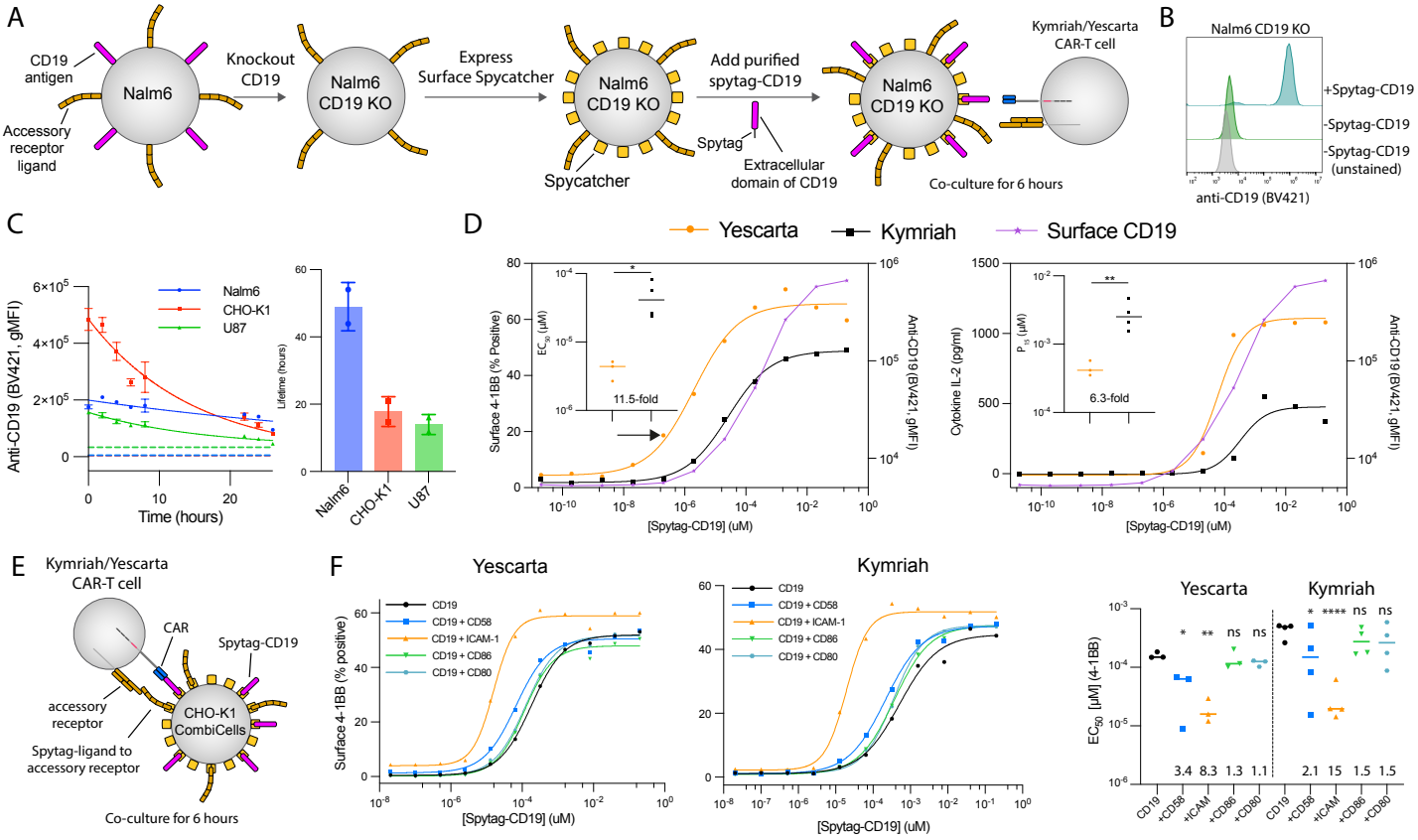

Figure 5: **Yescarta and Kymriah CAR-T cells can exploit LFA-1 but not CD2 or CD28 for improving their antigen sensitivity. (A)** Schematic of protocol for producing CD19^{-} hCD52-Spycatcher^{+} Nalm6 cells. **(B)** Surface level of Spytag-CD19 following coupling to hCD52-Spycatcher. **(C)** Representative timecourse of surface Spytag-CD19 on the indicated cell lines (left) and fitted lifetime from N=2 independent experiments (right). Horizontal dashed lines show unloaded controls. **(D)** A representative experiment showing T cell activation by 4-1BB (left) and supernatant IL-2 (right) with surface levels of CD19 on the target Nalm6 cell (right y-axes) and summary measures across N=3 (Yescarta) and N=4 (Kymriah) independent experiments (inset). **(E)** Schematic of CAR-T cell assay recognising CD19 alone or in combination with ligands to accessory receptors on CHO-K1 CombiCells. **(F)** A representative experiment showing T cell activation by 4-1BB (left, middle) and summary measures across N=3 (Yescarta) and N=4 (Kymriah) independent experiments (right). A paired t-test (D) or a t-test with Dunnett's multiple comparison correction (F) both on log-transformed values is used to determine p-values. Abbreviations: * = p-value$\leq$0.05, ** = p-value$\leq$0.01, *** = p-value$\leq$0.001, **** = p-value$\leq$0.0001.

The inhibitory ligand PD-L1 can inhibit CD2 and CD28 co-stimulation and the isolated recognition of pMHC

The accessory receptor PD-1 is known to inhibit T cell activation but it is presently debated whether it inhibits the TCR signalling, CD28 signalling, or both (13–16). Moreover, it is presently unknown whether PD-1 inhibits co-stimulation by other surface receptors, such as CD2. To investigate this, we used CHO-K1 CombiCells to stimulate CD8^{+} PD-1^{+} 1G4 TCR^{+} Jurkat T cells with pMHC alone or with different combinations of ligands to CD28 (CD80), CD2 (CD58) and PD-1 (PD-L1). As expected, ligands for CD28 or CD2 greatly increased T cell activation by pMHC (Fig. 6A-C). In contrast, the PD-1 ligand abolished T cell activation by TCR ligation alone as well as by simultaneous TCR and CD28 ligation. Interestingly, PD-

1 ligation also abolished T cell activation by TCR and CD2 ligation. These results could not be explained by PD-L1 coupling simply displacing pMHC, CD80, or CD58 because their surface levels were not reduced by coupling of PD-L1 (Fig. S7). While these data indicate that PD-1 ligation directly inhibits TCR signalling, they are also consistent with additional inhibitory effects on CD2 and CD28 signalling (Fig. 6D).

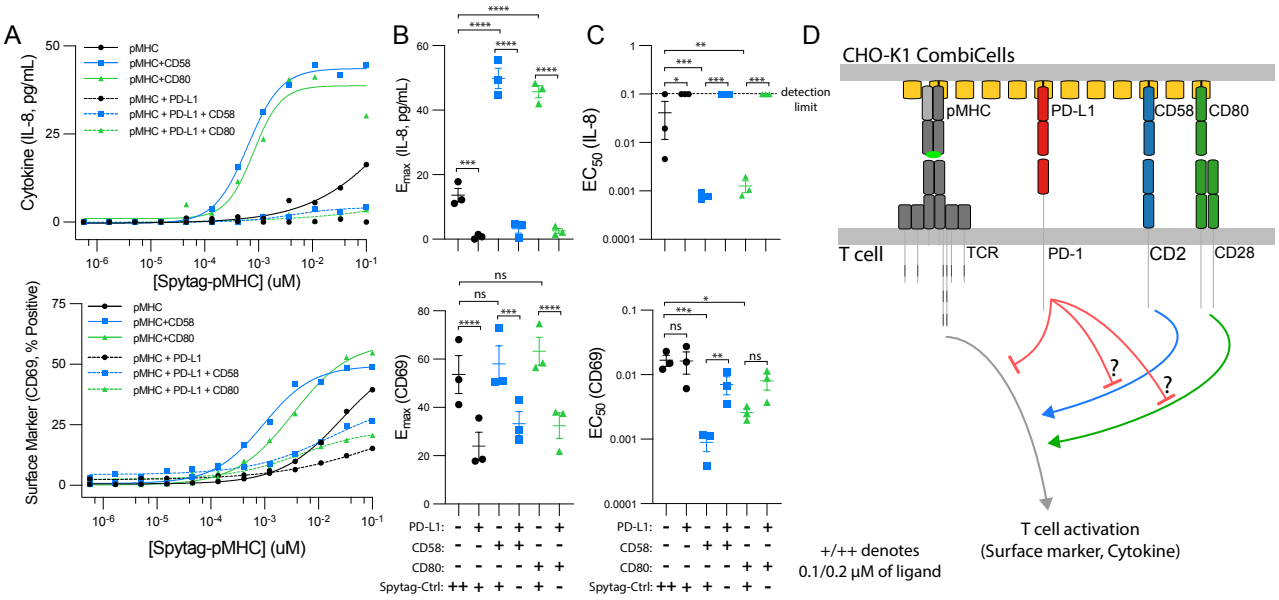

Figure 6: **Ligation of PD-1 inhibits T cell activation in response to pMHC alone or in combination with CD28 and CD2 co-stimulation.** Jurkat T cells transduced to express CD8, CD2, PD-1, and the 1G4 TCR were co-cultured with CHO-K1 CombiCells coupled with the indicated combinations of ligands for 20 hours. The protein CD19 fused to Spytag was used as placeholder control protein (Spy-Ctrl) to ensure that the total concentration of Spytag accessory receptor ligands remained constant (see Fig. S7 for surface levels). **(A)** Representative dose-response for IL-8 (top) and CD69 (bottom) and **(B,C)** fitted metrics across N=3 independent experiments. **(D)** Schematic of proposed inhibition mechanisms of PD-1. A t-test with Dunnett's multiple comparison correction directly (B) or on log-transformed values (C) is used to determine p-values. Abbreviations: * = p-value$\leq$0.05, ** = p-value$\leq$0.01, *** = p-value$\leq$0.001, **** = p-value$\leq$0.0001.

Discussion

We have developed a new Combicell platform for studying cell-cell recognition. It adapts the Spycatcher/Spytag split proteins system by expressing a novel membrane-anchored Spycatcher on the surface of cells selected and engineered to lack ligands under investigation. Soluble ligands fused to a membrane-proximal Spytag can readily be coupled to these cells in different combinations and concentrations. This platform, which we call Combicells, removes a major bottleneck that has been slowing down studies of cell-cell recognition.

CombiCell has several advantages over existing methods, which typically rely on genetic modifications coupled to cell sorting to produce many cell lines with different concentrations and combination of ligands. Firstly, it greatly reduces the number of cell lines. For example, testing all combinations of just 3 different ligands (e.g. antigen, costimulatory receptor ligand, and coinhibitory receptor ligand) at 8 different concentrations would require an impractical 6581 cell lines if current genetic methods were used. With Combicells

only one cell line is required. Secondly, cell lines grown independently in culture undergo genetic drift, making it difficult to rule out that observed differences are not the result of such changes. While this could be addressed by creating duplicate cell lines expressing each ligand combination, this would further increase the number of cell lines required. Thirdly, the use of CombiCell allows for generation of cells presenting different ligands within minutes whereas generating cell lines often takes weeks or months. Finally, titration allows ultra-low levels to be displayed on the target cell that are impossible to quantify by flow cytometry. This is crucial when investigating recognition by incredibly sensitive cells such as T cells, which can recognise a single antigen on a target cell (17, 18).

To exploit CombiCells, we have focused on T cell activation because T cells often interact with infected or cancerous cells that modulate expression of surface molecules to evade immune recognition. We have found that the adhesion receptor, CD2, produced a larger impact than LFA-1 and CD28 on both sensitivity and efficacy when T cells recognise pMHC antigens using their TCR. Interestingly, LFA-1 had the largest impact when T cells recognised the cancer antigen CD19 using the clinically approved Yescarta and Kymriah CAR-T cells. This suggests that CARs may be under-utilising a key adhesion receptor for antigen sensitivity. Consistent with a previous report, we found that Yescarta achieved higher antigen sensitivity compared to Kymriah (12).

The molecular mechanism of PD-1 inhibition has been shown to include direct and selective dephosphorylation of the cytoplasmic tail of CD28 (14, 19). We find that PD-1 engagement by PD-L1 can inhibit T cell activation in response to pMHC alone, suggesting that it can also dephosphorylate activatory tyrosines in the TCR signalling pathway (15, 16), as originally proposed (20). We also show that PD-1 can inhibit T cell activation enhanced by costimulation through CD2. While CD2 does not contain any tyrosines in its cytoplasmic tail, it has been shown to recruit the tyrosine-containing activatory kinase Lck (21). Our results, taken together with previous reports, are consistent with a model where PD-1 promiscuously inhibits many pathways involving tyrosine phosphorylation (22, 23).

While the Combicell platform has numerous advantages, it also has limitations. Firstly, because these Spycatcher-coupled ligands lack their native membrane/cytoplasmic domains, ligands whose function is influenced by these domains may behave differently. Secondly, even when initial surface densities are matched, the turnover of Spycatcher-coupled ligands is likely to differ from that of native ligands. Since the lifetime of Spytag-protein/Spycatcher complexes ranged from $\approx$7 hours (Fig. 2F) to $>$24 hours (Fig. 5C), additional ligand may need to be added for assays of long duration. Finally, this system is not suitable for capturing ligands with complex structures such as multiple transmembrane domains or polypeptide subunits.

By introducing CombiCells we have provided a platform that greatly facilitates the study of receptor/ligand interactions at cell/cell interfaces. We have utilized the platform to compare antigen sensitivity of TCRs and CARs and the contribution of various accessory receptors to T cell activation, including inhibitory receptors. This platform can be deployed to examine higher-order combinations of ligands, other surface receptors, and different cell types. Combicells enable analysis of ligand/receptor interactions at cellular interfaces with the same convenience that has hitherto been limited to those studying soluble ligand/receptor interactions. This platform should enhance our understanding of how cells integrate signals from diverse surface receptor/ligand interactions at cell-cell interfaces.

Acknowledgements

We thank Mark Howarth and Marion H. Brown for helpful discussions on the Spycatcher/Spytag system. We thank Vijay Kuchroo and Edward Greenfield for providing the anti-hamster ICAM-1 antibody. We thank Crystal Mackall and Robbie Majzner for providing the panel of Nalm6 cell lines with different levels of CD19. We thank Simon J. Davis for providing the TCR$^-$ Jurkat T cells.

Funding

The work was funded by a Wellcome Trust Senior Fellowship in Basic Biomedical Sciences (207537/Z/17/Z to OD), by a Biotechnology and Biological Sciences Research Council (BBSRC) studentship (BB/M011224/1 to AP), by a Wellcome Trust PhD Studentship in Science (108869/Z/15/Z to AMM), and by a Kennedy Trust for Rheumatology Research Professorship (to MLD).

Open access

This research was funded in whole, or in part, by the Wellcome Trust [207537/Z/17/Z]. For the purpose of Open Access, the author has applied a CC BY public copyright licence to any Author Accepted Manuscript version arising from this submission.

Author contributions

Conceptualization (OD), Data Curation (AP, VA, SBE, MB, ED, JP, AMM), Formal Analysis (AP, VA, SBE, MB, ED, AMM), Funding Acquisition (OD), Investigation (AP, VA, SBE, MB, ED, JP, AMM, MK, MLD, PAvDM, OD), Methodology (AP, VA, SBE, MB, ED, JP, JASF), Project Administration (OD), Supervision (MLD, PAvDM, OD), Visualization (AP, VA, SBE, MB, ED, JP, AMM), Writing – Original Draft (OD), Writing – Review & Editing (AP, VA, SBE, MB, JASF, MLD, PAvDM, OD)

Conflict of interest

AP, ED, JP, PAvdM, and OD have financial interests in a filed patent application related to CombiCells.

Materials & Methods

Protein Production & Purification

Production of Spytag-pMHC: HLA-A*02:01 heavy chain (UniProt residues 25–298) with a C-terminal Spytag003 and β_2-microglobulin were expressed as inclusion bodies in *E.coli*, refolded *in vitro* as described in (24) together with the 9V NY-ESO-1 peptide, and purified using size-exclusion chromatography on a Superdex S75 column (GE Healthcare, USA) in HBS-EP buffer (10 mM M HEPES pH 7.4, 150 mM NaCl, 3 mM EDTA, 0.005% v/v Tween-20).

Production of Spytag-ICAM-1/CD58/CD86/CD80/PD-L1/CD19: Cells were grown in Expi293™ Expression Medium (ThermoFisher Scientific, A1435101) in a 37°C incubator with 8% CO2 on a shaking platform at 130 rpm. Cells were passaged every 2–3 days with the suspension volume always kept below 33.3% of the total flask capacity. The cell density was kept between 0.5 and 3 million per ml. Before transfection cells were counted to check that cell viability was above 95%, and the density was adjusted to 3.0 million per ml. For 100 ml transfection, 320 µl ExpiFectamine™ 293 Transfection reagent (ThermoFisher Scientific, A14524) was mixed with 6 ml Opti-MEM (ThermoFisher Scientific, 31985062) for 5 min. During this incubation, 100 µg of expression plasmid was mixed with 6 ml Opti-MEM. The DNA was then mixed with the ExpiFectamine™ and incubated for 15 min before being added to the cell culture. One day after transfection 600 µl of enhancer 1 and 6 ml of enhancer 2 was added to the culture flask. The culture was returned to the shaking incubator for 4-5 days for protein expression to take place.

Cells were harvested by centrifugation and the supernatant collected and filtered through a 0.22 µm filter. Imidazole was added to a final concentration of 1 mM and PMSF added to a final concentration of 1 mM; 2 ml of Ni-NTA Agarose (Qiagen, 30310) was added per 50 ml of supernatant and the mix was left on a rolling platform at 4°C overnight. The mix was poured through a gravity flow column to collect the Ni-NTA Agarose. The Ni-NTA Agarose was washed three times with 10 ml of wash buffer (50 mM NaH2PO4, 300 mM NaCl, and 5 mM imidazole at pH 8). The protein was eluted with 15 ml of elution buffer (50 mM NaH2PO4, 300 mM NaCl, and 250 mM imidazole at pH 8). The protein was concentrated, and buffer exchanged into size exclusion buffer (25 mM NaH2PO4 and 150 mM NaCl at pH 7.5) using a protein concentrator with a 10,000 molecular weight cut-off. The protein was concentrated down to 500 µl and loaded onto a Superdex 200 10/300 GL (Cytiva, 17-5175-01) size exclusion column. Fractions corresponding to the desired peak were pooled and frozen at –80°C. Samples from all observed peaks were analysed on a reducing SDS–PAGE gel.

For purified Spytag-CD19, SUMO was used to stabilise the protein during production and therefore the HRV 3C Protease Solution Kit was used for SUMO removal (Pierce™, 88946). HRV protease was added to the purified protein at a pre-determined optimum ratio for full cleavage of the HRV site. The mixture was left overnight for full cleave to occur and then 1 ml of Glutathione Agarose (Pierce™, 16100) added for 4 hours to remove the protease. The solution was run through a gravity flow column to collect to SUMO plus protein of interest mixture. This was then added to 1 ml of Ni-NTA Agarose (Qiagen, 30310) and left on a rolling platform at 4°C overnight. The mix was poured through a gravity flow column to collect the Ni-NTA Agarose. The Ni-NTA Agarose was washed once with 10 ml of wash buffer (50 mM NaH2PO4, 300 mM NaCl, and 5 mM imidazole at pH 8). The protein was eluted with 15 ml of elution buffer (50 mM NaH2PO4, 300 mM NaCl, and 250 mM imidazole at pH 8). The protein was concentrated, and buffer exchanged into size exclusion buffer (25 mM NaH2PO4 and 150 mM NaCl at pH 7.5) using a protein concentrator with a 10,000 molecular weight cut-off and frozen in suitable aliquots at –80°C.

Generation of ICAM-1 knockout CHO-K1 cells

The expression of the hamster surface molecule ICAM1 was eliminated on CHO-K1 cells (ATCC CCL-61) using CRISPR/Cas9 lipofection, followed by lentiviral introduction of surface Spycatcher with the human CD52 hinge. Cells were maintained in DMEM (Sigma Aldrich) with 10% FCS (Sigma Aldrich). First, 200,000 were seeded overnight in a 6-well plate, followed by transfection with Lipofectamine CRISPRMAX Cas (Invitrogen), TrueCut Cas9 Protein v2 (Invitrogen), and an ICAM1 exon 2 (Ig domain 1)-targeting TrueGuide sgRNA (Invitrogen; sequence: CCACAGTTCTCAAAGCACAG) according to the manufacturer's U2OS protocol. Specifically, 125 µl OptiMEM (Thermo Fisher), 6.25 µg (37.5 pmol) Cas9, 3.75 µl of 10 µM sgRNA in TE (37.5 pmol), and 2.5 µl Lipofectamine Cas9 Plus were mixed in one tube. Separately, 125 µl OptiMEM, and 7.5 µl Lipofectamine CRISPRMAX were mixed and incubated for 1 min. Both tubes were combined and incubated for 15 min at RT. Finally, 50 µl of the solution was added per well of CHO cells. After 1 week, single clones were grown by performing limiting dilution.

Clones were screened using Sanger sequencing after genomic PCR. Specifically, gDNA from outgrown single cell clones was isolated using PureLink Genomic DNA Mini Kit (Invitrogen), amplified in a PCR with fwd primer AGGCATCAGATGGTGGCATTCT and rev primer GGTGTTTGGGGAGGGCAATACT, and submitted for Sanger sequencing. A clone which showed genomic editing was selected for further processing. Next, surface Spycatcher was introduced using high MOI lentiviral transduction, followed by single cell cloning using limiting dilution. The final clone selected showed high expression of surface SpyCatcher and absence of ICAM1 on the cell surface by flow cytometry. The expression of surface Spycatcher was assessed by coupling purified Spytag-mClover and flow cytometry. Specifically, 100k cells were incubated with 10 µM Spytag-mClover in PBS for 1 h at RT in the dark, washed in PBS, and acquired on a flow cytometer. ICAM1 expression was tested using unpurified Y5-3F9 hybridoma supernatant (provided by Vijay Kuchroo and Edward Greenfield). 100,000 cells were incubated with undiluted Y5 supernatant for 30 min on ice in the dark. Cells were washed in PBS and stained with 1:200 anti-mouse Alexa Fluor-488 secondary antibody for 30 min on ice in the dark. Finally, cells were washed and acquired on a flow cytometer.

sFCS measurements of diffusion

10^5 CHO-K1 cells expressing surface Spycatcher with different hinges were seeded in 8-well chambered coverslips (µ-Slide 1.5H, ibidi) overnight followed by labeling with 50 nM SpyTag-mClover3 for 30 minutes at 37°C. Cells were washed 2x in PBS and imaged in complete medium. Imaging was performed on a Zeiss LSM 780 inverted confocal microscope (Carl Zeiss) equipped with a 40x C-Apochromat NA 1.2 W FCS objective. mClover3 fluorescence was excited with a 488 nm Argon laser and collected onto hybrid GaAsP detectors (Channel S) using a 488 MBS with the pinhole set to 1 AU. The size of the observation area was calibrated using point-FCS measurements of a dye solution (Alexa Fluor 488, 20 nM) with a known diffusion coefficient (25), yielding an average ω of 214 nm. Diffusion coefficients (D) were then calculated using the equation $\omega^2 = D \times 4 \times t_{xy}$ where txy is the transit time. Line-scan FCS was performed by switching the ChS to photon-counting mode and data were collected at the basal cell membrane by acquiring a 52-pixel line (digital zoom 40x) at maximum scanning speed for 10^5 cycles. Files were saved as .lsm5 files and correlated externally using open-source FoCuS software (26).

Production of TCR or CAR transduced primary human CD8+ T cells

HEK 293T cells were seeded in DMEM supplemented with 10% FBS and 1% penicilin/streptomycin in 6-well plates to reach 60–80% confluency on the following day. Cells were transfected with 0.25 pRSV-Rev (Addgene, 12253), 0.53 μg pMDLg/pRRE (Addgene, 12251), 0.35 μg pMD2.G (Addgene, 12259), and 0.8 µg of transfer plasmid using 5.8 X-tremeGENE HP (Roche). Media was replaced after 16 hours and supernatant harvested after a further 24 hours by filtering through a 0.45 μm cellulose acetate filter. Supernatant from one well of a 6-well plate was used to transduce 1 million T cells.

Human CD8+ T cells were isolated from leukocyte cones purchased from the National Health Service's (UK) Blood and Transplantation service. Isolation was performed using negative selection. Briefly, blood samples were incubated with Rosette-Sep Human CD8+ enrichment cocktail (Stemcell) at 150μl/ml for 20 minutes. This was followed by a 3.1 fold dilution with PBS before layering on Ficoll Paque Plus (GE) at a 0.8:1.0 ficoll to sample ratio. Ficoll-Sample preparation was spun at 1200g for 20 minutes at room temperature. Buffy coats were collected, washed and isolated cells counted. Cells were resuspended in complete RMPI (RPMI supplemented with 10% v/v FBS, 100 penicillin, 100 streptomycin) with 50U of IL-2 (PeproTech) and CD3/CD28 Human T-activator Dynabeads (Thermo Fisher) at a 1:1 bead to cell ratio. At all times isolated human CD8+ T cells were cultured at 37 and 5% CO2. 1 million T cells in 1ml of media were subsequently transduced on the following day using lentivirus encoding for the 1G4 TCR, Kymriah CAR, or Yescarta CAR, per the section on lentiviral transduction. On days 2 and 4 post-transduction, 1ml of media was exchanged and IL-2 was added to a final concentration of 50U. Dynabeads were magnetically removed on day 5 post-transduction. When using the TCR, T cells were further cultured at a density of 1 million/ml and supplemented with 50U IL-2 every other day. When using CARs, T cells were further cultured at a density of 0.5 million/ml and supplemented with 100U IL-2 every other day. T cells were used between 10 and 16 days after transduction.

Production of Jurkat T cell line

The previously described TRAC$^{(-/-)}$TRBC$^{(-/-)}$ E6.1 Jurkat T cells (27) were successively transduced and sorted with lentivirus for the (i) 1G4 TCR, (ii) human CD8α-P2A-CD8β, (iii) human CD2, and (iv) human PD-1. Each transduction used 2 mL of crude lentivirus supernatant on $1x10^6$ Jurkat T cells and cells were allowed to rest for 48-96 h before being subjected to further operations. Jurkat T cells were sorted through FACS to obtain a highly enriched (>99.5%) population of CD8$^+$ PD-1$^+$ 1G4 TCR$^+$ CD2^{++} Jurkat T cells.

Coupling of ligands to CHO-K1 cells

50,000 CHO cells were seeded in a TC-coated 96-well flat-bottom plate and incubated overnight at 37C, 10% CO2. Spytag ligands were diluted to the required concentration in complete DMEM (10% FCS, 1% Penicillin-Streptomycin). Existing media was then removed from CHOs and diluted ligands added in a volume of 50μl, and incubated for 40 or 60 minutes at 37 C, 10% CO2. CHOs were then washed twice with complete DMEM.

Coupling of ligands to Nalm6 cells

30,000 Nalm6 cells were seeded in a TC-coated 96-well round bottom plate and incubated overnight at 37C, 5% CO2. On experiment day, Nalm6 cells were transferred into a TC-coated 96-well V-bottom plate and spun down for 5min at 520g. Spytag ligands were diluted to required concentration in complete RPMI (10%FCS, 1% Penicillin-Streptomycin). Existing media was removed from the Nalm6 cells and the diluted ligands added in a volume of 50μl, and incubated for 40 minutes at 37C, 5% CO2. Nalm6 cells were then washed twice with complete RPMI.

Co-culture assays with TCR or CAR transduced T cells

T cells were counted, and washed once in complete RPMI. 50,000 T cells in 200μl complete RPMI were added to CHO cells coupled with ligand in a 96-well flat-bottomed plate or to Nalm6 cells coupled with ligands and transferred into a 96-well round-bottomed plate. The cells were spun at 50g for 1 minute to ensure the T cells settle to the bottom of the plate and make contact with adherent CHO cells. The cells were then incubated at 37C, 5% CO2 for 6 hours (primary T cells) or 20 hours (Jurkat T cells).

Flow cytometry - Detection of ligands

Straight after ligand coupling and subsequent washing, 10mM EDTA was added to the CHO cells to detach them. The cells were transferred to a v-bottom plate and spun for 5 minutes at 500g, 4C. The cells were washed once with PBS-BSA 1% for 5 minutes at 500g, 4C. To detect ligands, fluorescently conjugated antibodies against proteins of interest were diluted in PBS-BSA (1%), at a 1:200 dilution and added at a volume of 50 μl to CHO cells. The cells were resuspended and incubated for 20 minutes at 4C in the dark. The cells were washed twice in PBS, and resuspended in 75 μl PBS, before running on a flow cytometer.

Flow cytometry - Detection of T cell activation

At the end of the stimulation assay, the supernatant was carefully removed and saved for ELISA analysis. 10mM EDTA in PBS was then added to detach the T cells and CHOs. The cells were then aspirated and transferred to a v-bottom plate and washed once in 200μl PBS 1% BSA (500g, 4C, 5 minutes). Antibodies against T cell activation markers were diluted in PBS 1% BSA at a 1:200 dilution. An anti-CD45 antibody was used to selectively stain T cells and distinguish them from CHO cells during flow cytometry analysis. To detect TCR/CAR expression fluorescently-conjugated peptide-MHC tetramers were added to the staining antibodies at a 1:1000 dilution. A viability dye was also added at a dilution if 1:2500 to distinguish live cells from dead cells. 50μl of this staining solution was to the cells, before incubating them for 20 minutes at 4C in the dark. The cells were washed twice in PBS, and resuspended in 75μl PBS, before running on a flow cytometer. Flow cytometry data was analysed using FlowJo (BD Biosciences).

Cytokine detection

IL-2 Human uncoated ELISA kit, TNF-α Human uncoated ELISA kit, IFN-γ Human uncoated ELISA kit, or IL-8 Human uncoated ELISA kit and Nunc MaxiSorp 96-well plates were used according to the manufacturer's instructions. The supernatant from stimulation assays were either undiluted (IL-8) or diluted (all other cytokines) prior to ELISAs. The absorbance at 450 nm and 570nm were measured using a SpectraMax M5 plate reader (Molecular Devices).

Reagents

Expi293™: Expression Medium ThermoFisher Scientific Lot: A1435101 ExpiFectamine™ 293 Transfection reagent ThermoFisher Scientific Lot: A14524 Opti-MEM ThermoFisher Scientific Lot: 31985062 Ni-NTA Agarose Qiagen lot: 30310 Glutathione Agarose Pierce™ Lot: 16100 Superdex 200 10/300 GL Cytiva Lot: 17-5175-01 HRV 3C Protease Solution Kit Pierce™ Lot: 88946 DMEM: Thermo Scientific Lot: 41966029 RPMI Thermo Scientific: Lot: 21875034 EDTA: UltraPure 0.5M EDTA, pH 8.0: Invitrogen Lot: 15-575-020 BSA: Sigma-Aldrich Lot: A7906-500G IL-2 Human uncoated ELISA kit: Invitrogen Lot: 88-7025-77 TNF-α Human uncoated ELISA kit: Invitrogen Lot: 88-7346-77 IFN-γ Human uncoated ELISA kit: Invitrogen Lot: 88-7316-77 Nunc MaxiSorp 96-well plates Thermo Fisher Scientific Lot: 442404

Antibodies for Flow Cytometry (all from BioLegend):

CD58 Clone: TS2/9 Fluorophore: APC Catalog: 330918

ICAM-1 Clone: HCD54 Fluorophore: AF647 Catalog: 353114

CD86 Clone: Fluorophore: FITC Catalog: 374203

CD80 Clone: 2D10 Fluorophore: BV421 Catalog: 305221

HLA-A2 Clone: BB7.2 Fluorophore: PE Catalog: 343306

CD69 Clone: FN50 Fluorophore: AF488 Catalog: 310916

4-1BB Clone: 4B4-1 Fluorophore: AF647 Catalog: 309824

CD45 Clone: HI30 Flurophore: BV510 Catalog: 304036

Zombie NIR Fixable Viability Kit Catalog: 423105

Data analysis

EC_{50} is calculated as the concentration of antigen required to elicit 50% of the maximum response determined for each condition individually whereas P_X is calculated as the concentration of antigen required to elicit X% of the maximum activation determined by the pMHC alone condition.

Surface Spycatcher Sequences

Format: IgK signal sequence-Spycacher003 sequence-flexible linker sequence-extracellular hinge sequence-transmembrane sequence-cytoplasmic sequence

mCD80: METDTLLLWVLLLWVPGSTGD- VTTLSGLSGEQGPSGDMTTEEDSATHIKFSKRDEDGRELAGAT-MELRDSSGKTISTWISDGHVKDFYLYPGKYTFVETAAPDGYEVATPIEFTVNEDGQVTVDGEATEGDAHT-GSSGSGGS-HVSEDFTWEKPPEDPPDSKN-TLVLFGAGFGAVITVVVIVVII-KCFCKHRSCFRRNEASRETNNSLTFGPEEALAEQTVFL

mCD80-Short: METDTLLLWVLLLWVPGSTGD- VTTLSGLSGEQGPSGDMTTEEDSATHIKFSKRDEDGRE-LAGATMELRDSSGKTISTWISDGHVKDFYLYPGKYTFVETAAPDGYEVATPIEFTVNEDGQVTVDGEATEGDAHT-GSSGSGGS-PPDSKN-TLVLFGAGFGAVITVVVIVVII-KCFCKHRSCFRRNEASRETNNSLTFGPEEALAEQTVFL

hCD52-Short: METDTLLLWVLLLWVPGSTGD- VTTLSGLSGEQGPSGDMTTEEDSATHIKFSKRDEDGRE-LAGATMELRDSSGKTISTWISDGHVKDFYLYPGKYTFVETAAPDGYEVATPIEFTVNEDGQVTVDGEATEGDAHT-GSSGSGGS-TSQTSSPSASSNISGGIFLFFVANAIIHLFCFS (TSQTSSPS remains in the mature protein)

References

1. Belardi B, Son S, Felce JH, Dustin ML, Fletcher DA (2020) Cell-cell interfaces as specialized compartments directing cell function. *Nature Reviews Molecular Cell Biology*.

2. Chen L, Flies DB (2013) Molecular mechanisms of T cell co-stimulation and co-inhibition. *Nature Reviews Immunology* 13:227–242.

3. Majzner RG, Mackall CL (2018) Tumor antigen escape from car t-cell therapy. *Cancer Discovery* 8:1219–26.

4. Abdul Razak F, Diepstra A, Visser L, van den Berg A (2016) CD58 mutations are common in Hodgkin lymphoma cell lines and loss of CD58 expression in tumor cells occurs in Hodgkin lymphoma patients who relapse. *Genes and Immunity* 17:363–366.

5. Wang ECY, et al. (2018) Suppression of costimulation by human cytomegalovirus promotes evasion of cellular immune defenses. *Proceedings of the National Academy of Sciences* 115:4998–5003.

6. Larson RC, et al. (2022) CAR T cell killing requires the IFNγR pathway in solid but not liquid tumours. *Nature* 604:563–570.

7. Keeble AH, Howarth M (2020) Power to the protein: enhancing and combining activities using the Spy toolbox. *Chemical Science* 11:7281–7291.

8. Milstein O, et al. (2008) Nanoscale increases in CD2-CD48-mediated intermembrane spacing decrease adhesion and reorganize the immunological synapse. *Journal of Biological Chemistry* 283:34414–34422.

9. Pettmann J, et al. (2021) The discriminatory power of the t cell receptor. *eLife* 10:1–42.

10. Maus MV, et al. (2016) An MHC-restricted antibody-based chimeric antigen receptor requires TCR-like affinity to maintain antigen specificity. *Molecular Therapy — Oncolytics* 3:16023.

11. Haso W, et al. (2012) Anti-CD22-chimeric antigen receptors targeting B cell precursor acute lymphoblastic leukemia. *Blood* 121:1165–1174.

12. Majzner RG, et al. (2020) Tuning the antigen density requirement for car T-cell activity. *Cancer Discovery* 10.

13. Kamphorst AO, et al. (2017) Rescue of exhausted CD8 T cells by PD-1–targeted therapies is CD28-dependent. *Science* 355:1423–1427.

14. Hui E, et al. (2017) T cell costimulatory receptor CD28 is a primary target for PD-1–mediated inhibition. *Science* 355:1428–1433.

15. Mizuno R, et al. (2019) PD-1 primarily targets TCR signal in the inhibition of functional T cell activation. *Frontiers in Immunology* 10:1–14.

16. Celis-Gutierrez J, et al. (2019) Quantitative Interactomics in Primary T Cells Provides a Rationale for Concomitant PD-1 and BTLA Coinhibitor Blockade in Cancer Immunotherapy. *Cell Reports* 27:3315–3330.

17. Huang J, et al. (2013) A Single Peptide-Major Histocompatibility Complex Ligand Triggers Digital Cytokine Secretion in CD4+ T Cells. *Immunity* pp 1–12.

18. Siller-Farfán JA, Dushek O (2018) Molecular mechanisms of T cell sensitivity to antigen. *Immunological Reviews* 285:194–205.

19. Xu X, et al. (2020) PD-1 and BTLA regulate T cell signaling differentially and only partially through SHP1 and SHP2. *The Journal of cell biology* 219.

20. Freeman GJ, et al. (2000) Engagement of the PD-1 immunoinhibitory receptor by a novel B7 family member leads to negative regulation of lymphocyte activation. *The Journal of experimental medicine* 192:1027–1034.

21. Beyers AD, Spruyt LL, Williams AF (1992) Molecular associations between the T-lymphocyte antigen receptor complex and the surface antigens CD2, CD4, or CD8 and CD5. *Proceedings of the National Academy of Sciences* 89:2945–2949.

22. Clemens L, et al. (2021) Determination of the molecular reach of the protein tyrosine phosphatase SHP-1. *Biophysical Journal* 120:2054–2066.

23. Boussiotis VA (2016) Molecular and Biochemical Aspects of the PD-1 Checkpoint Pathway. *New England Journal of Medicine* 375:1767–1778.

24. Aleksic M, et al. (2010) Dependence of T cell antigen recognition on T cell receptor-peptide MHC confinement time. *Immunity* 32:163–74.

25. Petrášek Z, Schwille P (2008) Precise measurement of diffusion coefficients using scanning fluorescence correlation spectroscopy. *Biophysical Journal* 94:1437–1448.

26. Waithe D, et al. (2018) Optimized processing and analysis of conventional confocal microscopy generated scanning FCS data. *Methods* 140-141:62–73.

27. Chen KY, et al. (2021) Trapping or slowing the diffusion of T cell receptors at close contacts initiates T cell signaling. *Proceedings of the National Academy of Sciences of the United States of America* 118:e2024250118.

Supplementary Information
Using CombiCells, a platform enabling titration and combinatorial display of cell surface ligands, to investigate the sensitivity and costimulatory requirements of TCRs and CARs

Ashna Patel[1], Violaine Andre[1], Sofia Bustamante Eguiguren[1], Michael I. Barton[1], Eleanor M. Denham[1*], Johannes Pettmann[1†], Alexander M Mørch[2], Mikhail A. Kutuzov[1], Jesús A. Siller-Farfán[1], Michael L. Dustin[2], P. Anton van der Merwe[1], Omer Dushek[1,¶]

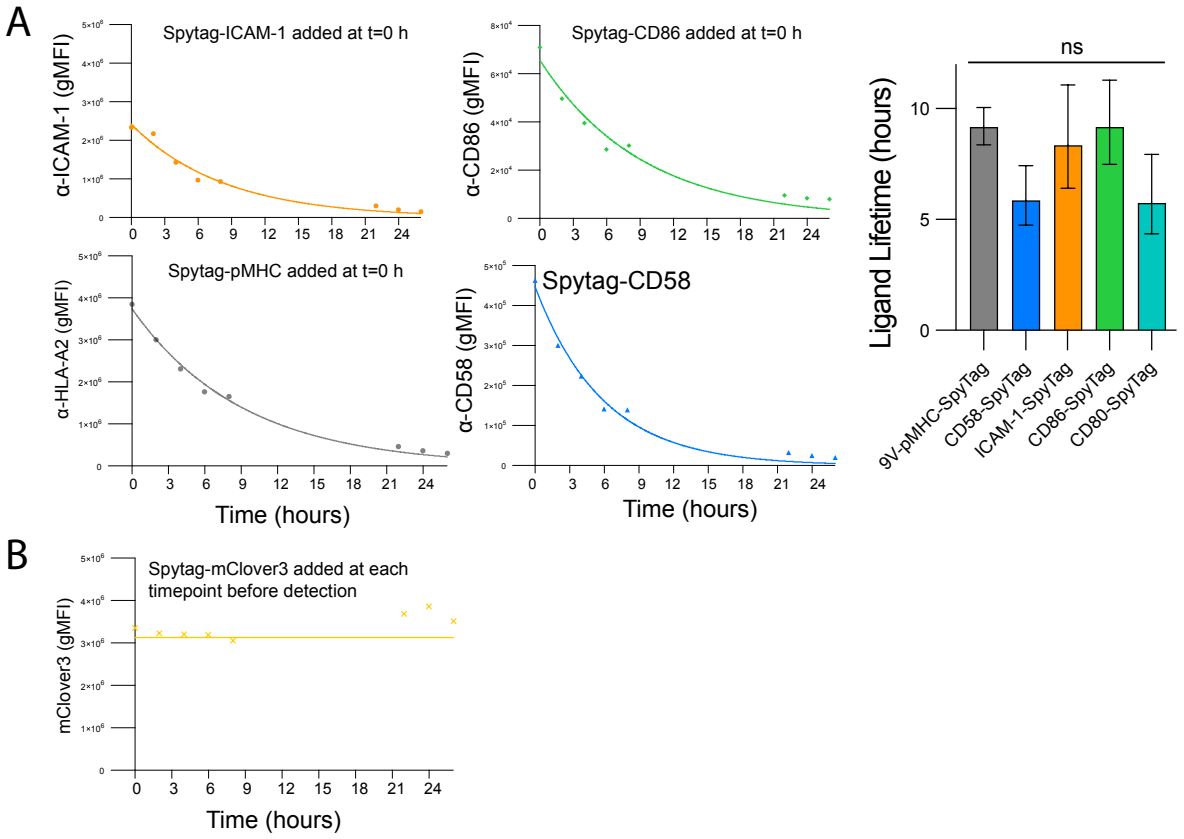

Figure S1: **Lifetime of Spytag-ligands coupled to surface Spycatcher on CombiCells detected using ligand-specific antibodies**. **(A)** The indicated ligand was coupled ([ligand] = 0.5 μM) and detected using a conformational specific antibody in flow cytometry (left). An exponential fit produced an estimate for the ligand lifetime (right). **(B)** The total surface level of Spycatcher was detected at each time point by coupling Spytag-mClover3 at each time point immediately before flow cytometry.

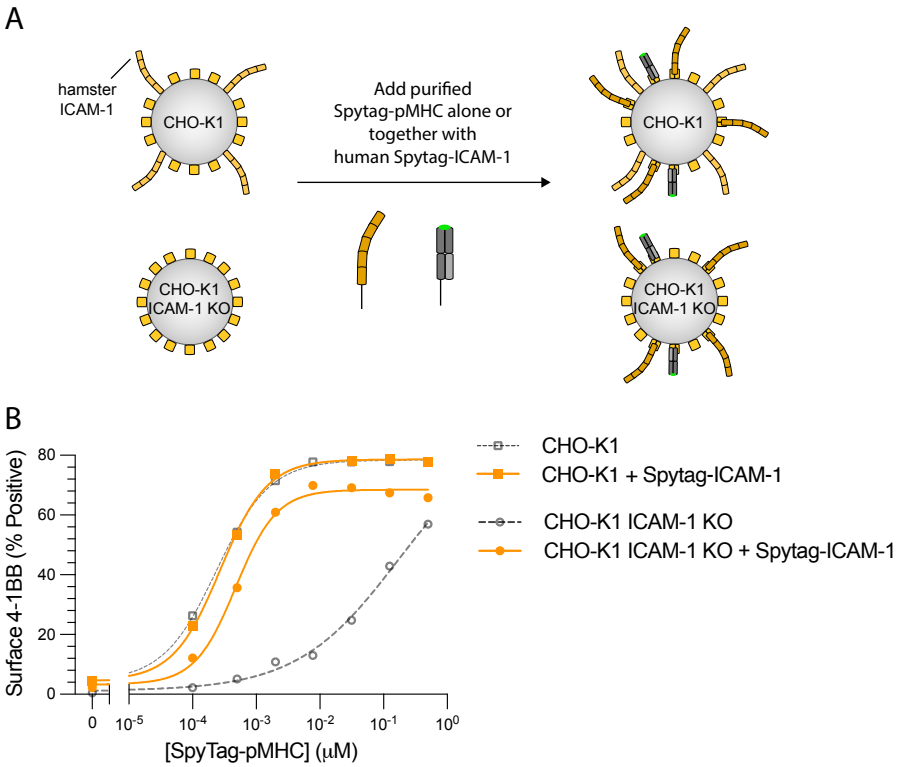

Figure S2: **T cells can exploit endogenously expressed hamster ICAM-1 or exogenous human Spytag-ICAM-1 when recognising Spytag-pMHC. (A)** Schematic of CHO-K1 cell lines used. **(B)** T cell activation measured by the surface marker 4-1BB in response to Spytag-pMHC alone or in combination with 0.5 μM of Spytag-ICAM-1 on the indicated CHO-K1 cell line.

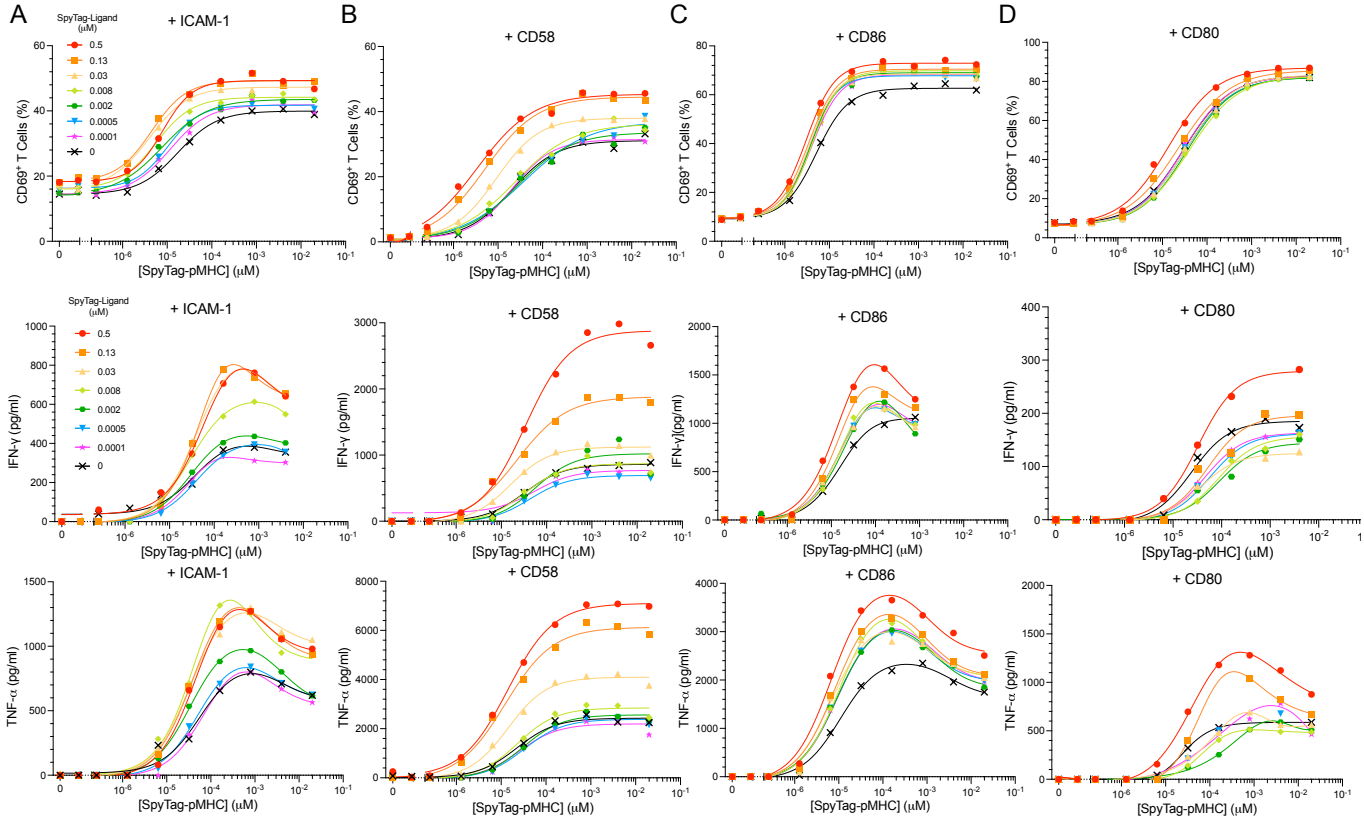

Figure S3: **Additional measures of T cell activation (related to Fig. 3).**

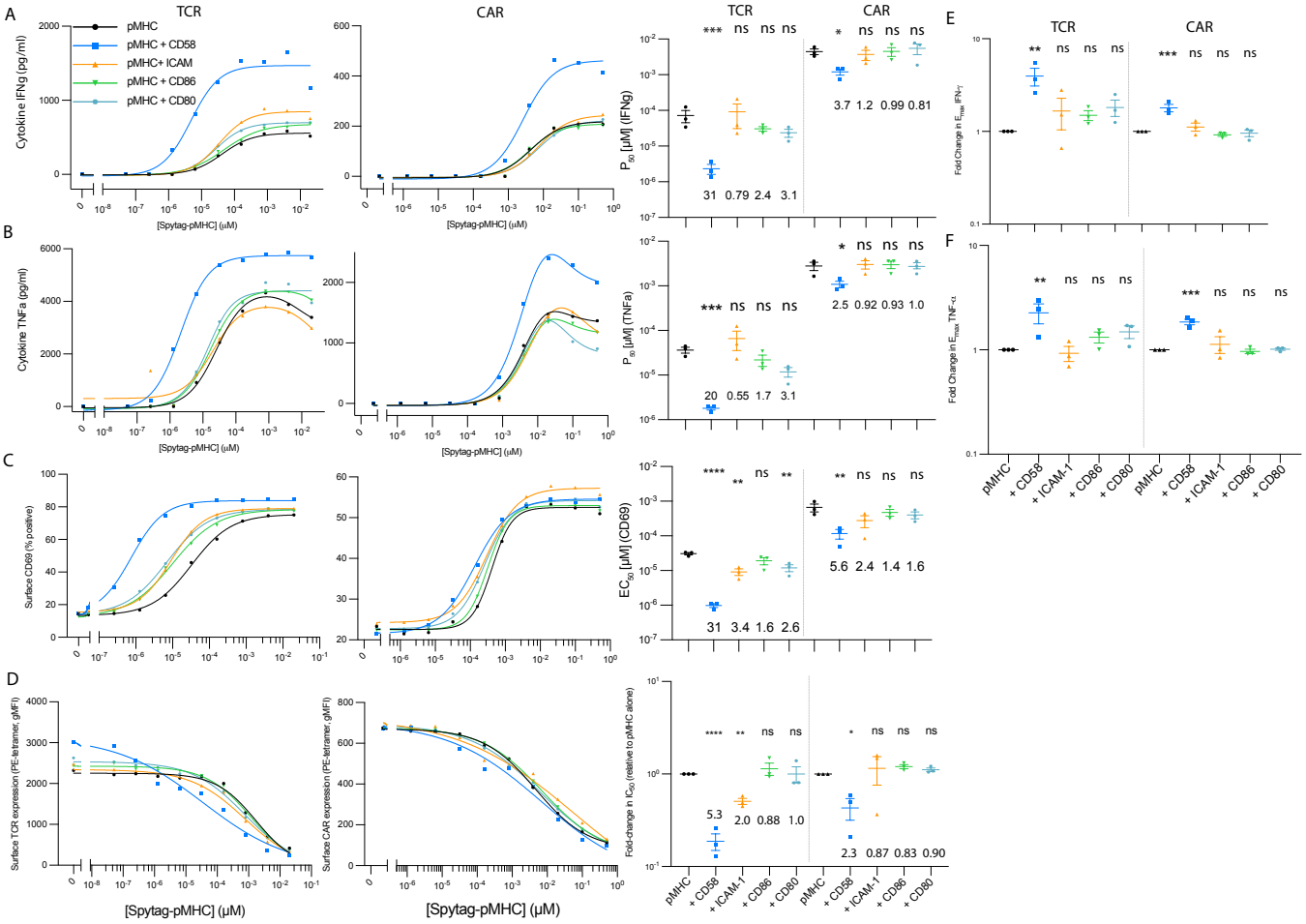

Figure S4: **Additional measures of T cell activation (related to Fig. 4).** Representative dose-response for the TCR and CAR (left) and summary measures of antigen sensitivity for N=3 independent experiments (right) for **(A)** IFN-γ, **(B)** TNF-α, **(C)** surface CD69, and **(D)** surface antigen receptor. **(E,F)** The fold-change in the maximum (E) IFN-γ and (F) TNF-α relative to pMHC antigen alone. A t-test with Dunnett's multiple comparison correction on log-transformed values is used to determine p-values. Abbreviations: * = p-value$\leq$0.05, ** = p-value$\leq$0.01, *** = p-value$\leq$0.001, **** = p-value$\leq$0.0001.

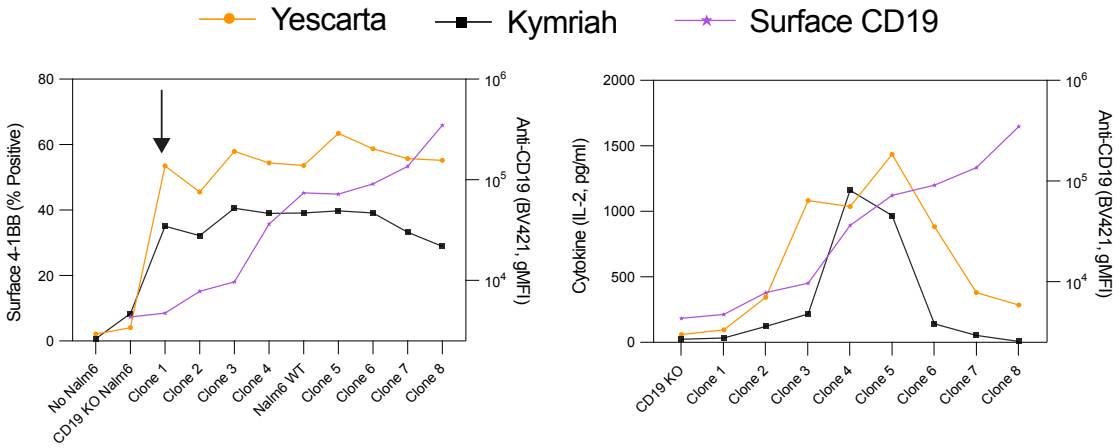

Figure S5: **CAR-T cells recognising CD19 endogenously expressed at different levels on the surface of a panel of Nalm6 cell lines.** Primary human CD8$^+$ T cells were co-cultured with each Nalm6 line for 6 hours before T cell activation was assessed by surface 4-1BB (left) and the supernatant levels of IL-2 (right). The complete activation of 4-1BB is observed in response to the Nalm6 cell line expressing the lowest level of CD19 (Clone 1, see right y-axes for CD19 level on each Nalm6 cell line). Representative experiment out of 2 independent experiments is shown.

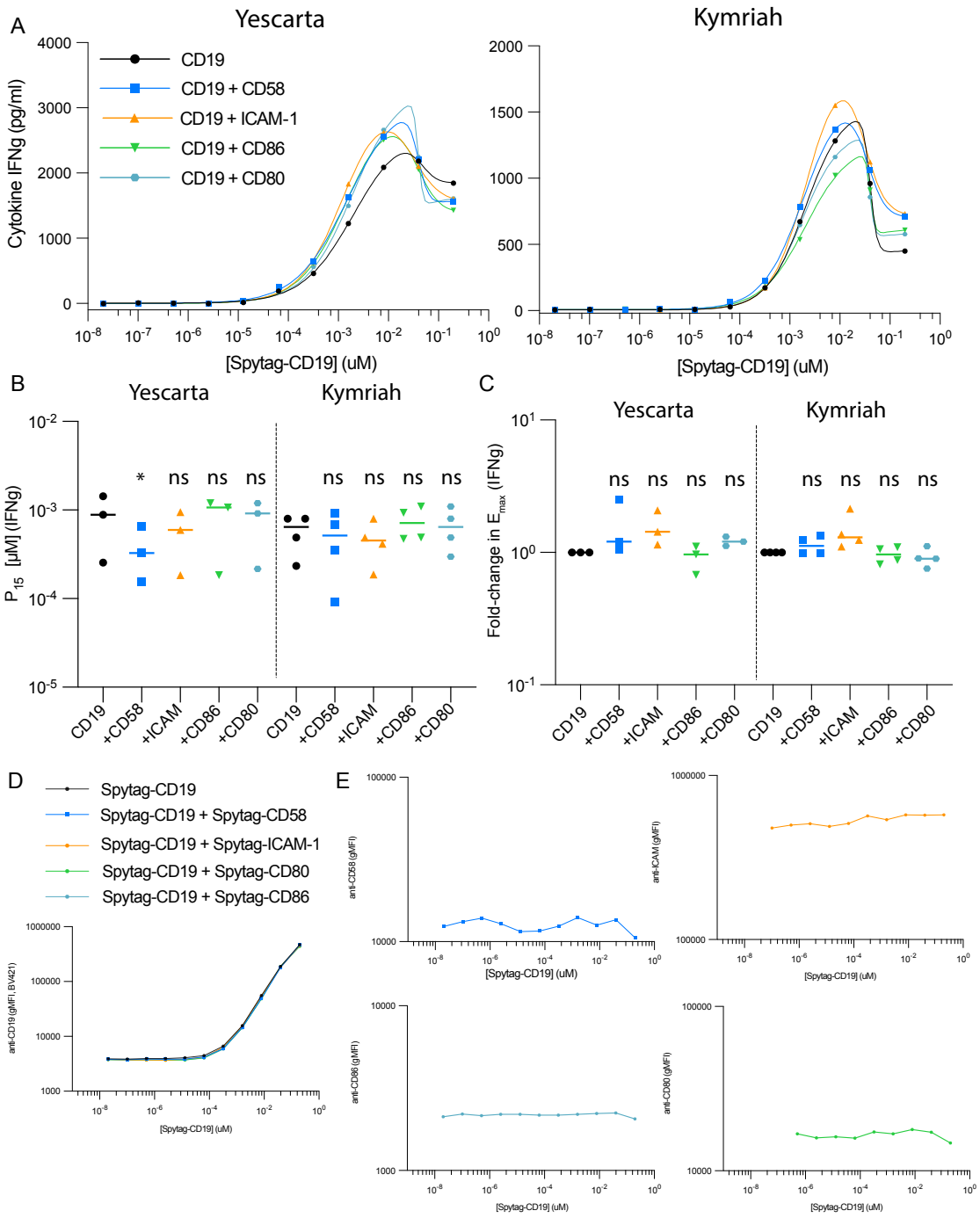

Figure S6: **Cytokine production by CD19-targeting CAR-T cells is largely independent of accessory receptors (Related to Fig. 5E-F). (A-C)** Cytokine production and **(D,E)** ligand loading data for the 7 independent experiments (3 for Yescarta and 4 for Kymriah) described in Fig. 5E-F. **(A)** Representative dose-response showing a model fit (solid line) used to estimate **(B)** the concentration of Spytag-CD19 required to elicit 15% of the maximal cytokine level (P_{15}) and **(C)** the maximal cytokine level (shown as a fold-change relative to Spytag-CD19 alone). A one-way ANOVA with Sidak's multiple comparison correction was used to determine p-values. Abbreviations: * = p-value$\leq$0.05. **(D)** Surface levels of Spytag-CD19 and **(E)** each Spytag-ligand on CHO-K1 CombiCells showing that Spytag-ligands do not impact Spytag-CD19 and vice versa. Representative surface levels out of 7 independent experiments. The concentration of each Spytag-ligand is 0.1 μM and the concentration of Spytag-CD19 as indicated on the x-axes.

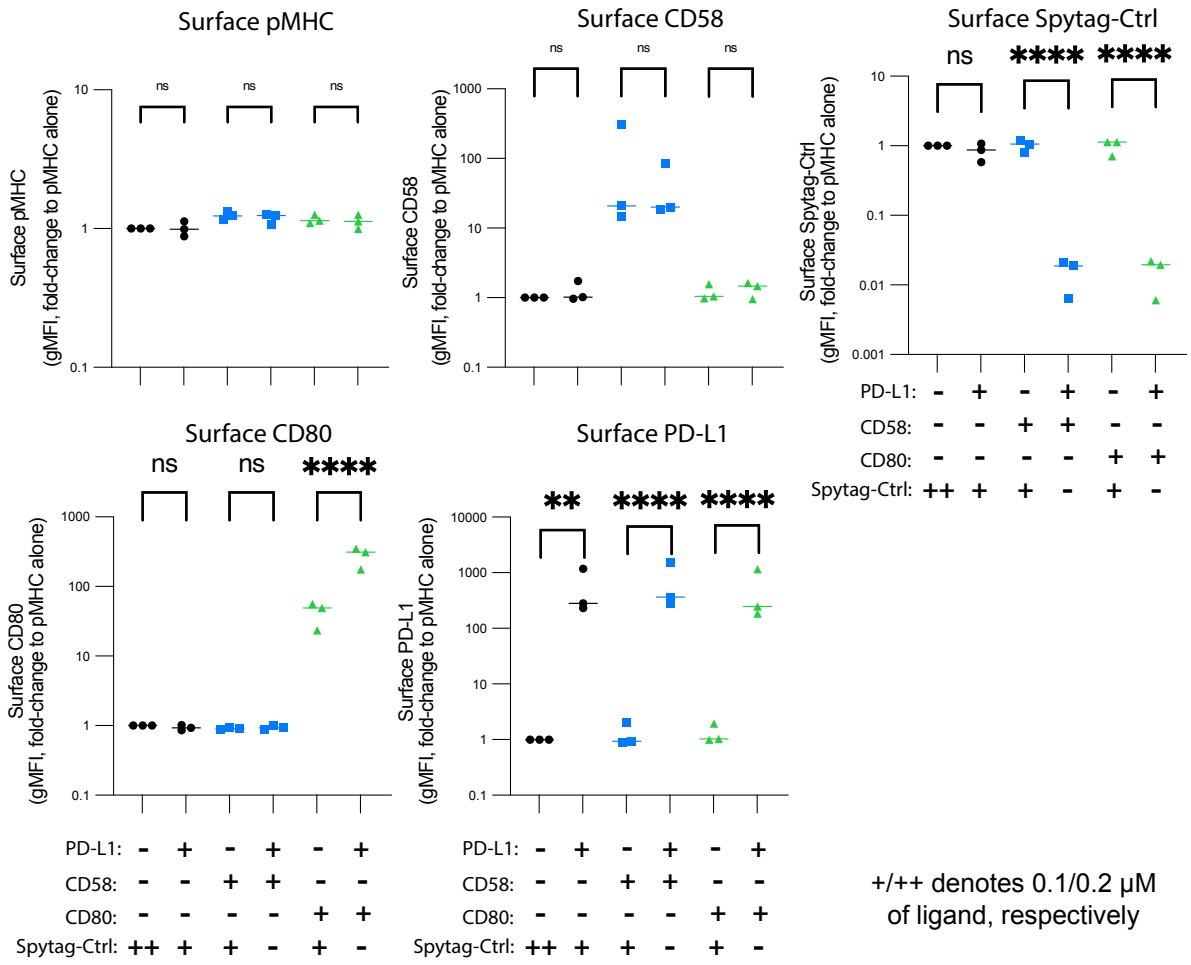

Figure S7: **Coupling of PD-L1 does not reduce the coupling of pMHC or other ligands, and vice versa, on CHO-K1 CombiCells.** CHO-K1 CombiCells were coupled with 0.1 μM of the indicated ligands and surface expression of each ligand was detected using antibodies in flow cytometry. The concentration of pMHC in all panels is 0.1 μM and data is presented as fold-changes relative to the gMFI of the pMHC alone condition (first column without PD-L1, CD58, or CD80). The protein CD19 fused to Spytag (Spytag-Ctrl) was added so that the total concentration of additional ligand was always 0.2 μM. A one-way ANOVA with Sidak's multiple comparison correction was used to determine p-values. Abbreviations: * = p-value$\leq$0.05, ** = p-value$\leq$0.01, *** = p-value$\leq$0.001, **** = p-value$\leq$0.0001